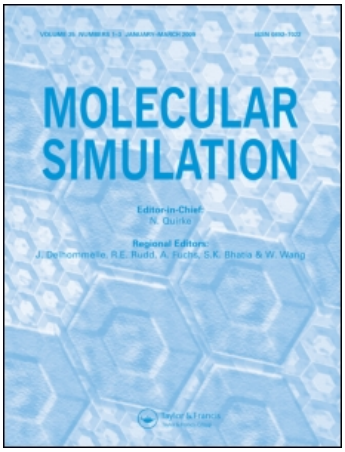

Molecular Simulation
Publication details, including instructions for authors and subscription information:
http://www.informaworld.com/smpp/title~content=t713644482

A computational H5N1 neuraminidase model and its binding to commercial drugs

P. Nimmanpipug[a]; J. Jitonnom[a]; C. Ngaojampa[a]; S. Hannongbua[b]; V. S. Lee[a]
[a] Department of Chemistry, Faculty of Science, Chiang Mai University, Chiang Mai, Thailand [b] Department of Chemistry, Faculty of Science, Chulalongkorn University, Bangkok, Thailand

To cite this Article Nimmanpipug, P. , Jitonnom, J. , Ngaojampa, C. , Hannongbua, S. and Lee, V. S.(2007) 'A computational H5N1 neuraminidase model and its binding to commercial drugs', Molecular Simulation, 33: 6, 487 — 493
To link to this Article: DOI: 10.1080/08927020701255862
URL: http://dx.doi.org/10.1080/08927020701255862

Molecular Simulation, Vol. 33, No. 6, May 2007, 487–493

Taylor & Francis
Taylor & Francis Group

A computational H5N1 neuraminidase model and its binding to commercial drugs

P. NIMMANPIPUG†, J. JITONNOM†, C. NGAOJAMPA†, S. HANNONGBUA‡ and V. S. LEE†*

Department of Chemistry, Faculty of Science, Chiang Mai University, Chiang Mai, 50200 Thailand
Department of Chemistry, Faculty of Science, Chulalongkorn University, Bangkok, 10330 Thailand

(Received August 2006; in final form January 2007)

In order to understand the mechanisms of ligand binding and interaction between two commercial drugs (ligands), zanamivir and oseltamivir and H5N1 Influenza Virus Neuraminidase subtype N1, a three-dimensional model of N1-ligand (GenBank accession no. AAS654617) was initially generated by homology modeling using the 13 high-resolution X-ray structures of neuraminidase N2 and N9 as the template. With the aid of the molecular mechanics and molecular dynamics methods, the final implicit solvent refined model was obtained. It was, then, assessed by PROCHECK, PROSA and VERIFY3D. With this model, a flexible docking study was performed. The results show strong hydrogen bond interactions between the glycerol side chains of zanamivir and Arg29 of the N1. Common hydrogen bonds between the carboxyl groups and Arg279 were found for both drugs. It was also found that the Glu30, Asp62, Arg63, Arg204, Trp310, Tyr313, Glu336, Ile338, Trp348, Ala349 were observed to facilitate the enzyme-ligand non-bonding interactions as they are located within the radius of 5 Å from all atoms of both drugs. Charge distribution was evaluated using the semi-empirical AM1 method. The results show that the total net charges of the —NH side chain of zanamivir is less negative than that of oseltamivir. This is in contrast to what is observed for the amide and alkyl (ether/glycerol) side chains. In comparison of the binding free energies between the X-ray N2-ligand and N9-ligand complexes, N1-ligand binding is found to be less potent than N2 and N9 subtypes, while N2-ligand and N9-ligand are roughly comparable. In addition, it is interesting to observe that the binding free energies for all three subtypes of the zanamivir complexes are lower than those of oseltamivir.

Keywords: H5N1; Avian influenza; Molecular dynamics simulations; Structure refinement; Flexible docking

1. Introduction

The transmission of avian H5N1 influenza viruses from chicken to 18 humans in Hong Kong in 1997 with six deaths established that avian influenza viruses can transmit to and cause lethal infection in humans [1]. By November 9th, 2005, there were a total of 125 confirmed human cases of the H5N1 virus infection, 64 of which were fatal, according to the world health organization (WHO). Since the start of the year 2006, bird flu has re-emerged in Indonesia's main island of Java and South Sulawesi province. Preliminary analysis of the virus has not shown any new mutations, which should indicate and increase ability to be transmitted between humans. The high death rate and high resistance to most commercially available drugs against influenza [2,3] causes a great concern worldwide. So far, oseltamivir (commercially named "Tamiflu") and zanamivir (commercially named "Relenza"), neuraminidase inhibitors, are the only two effective drugs for the protean pandemic threat of H5N1 influenza.

Influenza is caused by three related viruses: influenza A, B or C. While B and C are mostly found in humans, the A virus can cross the species barrier and abruptly change its genetic blueprint. Infection is more severe and deadly worldwide outbreaks can occur. All known avian influenza viruses are classified as type A. Further subtyping of influenza A viruses is based on antigenic glycoprotein enzymes found on the surface of virus; Hemagglutinin (HA) and neuraminidase (NA). To date, 16 HA subtypes (H1–H16) and nine NA subtypes (N1–N9) of influenza A viruses have been identified [1]. NA has become the main target for drug design against influenza. The inhibition of NA can delay the release of progeny virus from the surface

*Corresponding author. Tel.: + 66-53-943341-5. Ext. 117. Fax: + 66-53-892277. Email: vannajan@chiangmai.ac.th

Molecular Simulation
ISSN 0892-7022 print/ISSN 1029-0435 online © 2007 Taylor & Francis
http://www.tandf.co.uk/journals
DOI: 10.1080/08927020701255862

of infected cells [4] so as to suppress the viral population and allow time for the host immune system to eliminate the virus. Several successful drugs have been developed based on the crystal structure of NA. However, some of the H5N1 strains bear high resistance for existing NA inhibitors. To understand the drug-resistance of H5N1 virus at a deeper level, a structure–activity relationship for some existing NA inhibitors is an emergent research topic for the next possible pandemic influenza.

As the experimental structural data for H5N1 neuraminidase is not available so far, we attempt to build N1 neuraminidase from the human influenza H5N1 viruses (A/Thailand/2(SP33)/2004(H5N1)) isolated from Thailand [5]. In this study, a homology model of N1-NA was built according to the crystal structure of N2-NA and N9-NA complexed with two commercial drugs, zanamivir and oseltamivir. Subsequently, the structure–activity relationship was studied based on the modeled complex structure of H5N1-NA with the two drugs. Finally, the drug-resistance of H5N1 influenza was analyzed and some insights were gained that might lead to new information to solve the drug-resistance problem.

2. Computational details

2.1 H5N1-NA model built

The sequence of N1-NA (accession no. AAS654617) that was obtained from the National Center for Biotechnology Information (NCBI, http://www.ncbi.nlm.nih.gov/) contains 457 amino acids. Totally 13 templates with high resolution values (>2.00 Å) of N2 (PDB code: 1inhA, 1ingA, 1inw, 1ivf, 1ivg, 1nn2 and 2bat) and N9 (PDB code: 1NNB, 1NNA, 7NN9, 1NNC, 1L7FA and 1MWE) neuraminidase were chosen from the Research Collaboratory for Structural Bioinformatics Protein Data Bank (http://www.rcsb.org/pdb) as templates for homology modeling. Multiple sequence alignments were derived from ClustalX 1.83 [6]. The rough 3D model based on multiple templates was constructed using the academic version of MODELLER 8.1 [7]. The model with the lowest objective function was chosen as the best proposed model (model A) and used for further refinements to include all missing atoms especially hydrogen atoms followed by energy minimization and to include the solvent effect by implicit solvent molecular dynamics (MD) simulations using the generalized born (GB) model at 300 K for 500 ps with a time step of 2.0 fs using AMBER 8.0 force field parameter03 [8,9]. The overall quality of the refined model was evaluated by utilizing PROCHECK [10] for a evaluation of Ramachandran plot quality, PROSA [11] for interaction energy testing and VERIFY3D [12] for assessing the compatibility of each amino acid residue.

2.2 Flexible docking study

Further flexible molecular dockings [13] with Genetic Algorithm was performed using BioMedCache 2.0 Software [14] to find the most favorable binding interaction. Two drugs, oseltamivir and zanamivir, were docked into the binding site of H5N1-NA model yielded from Section 2.1. The structure of zanamivir was obtained from X-ray crystallographic complex structure (PDB ID: 1A4G) [15], whereas oseltamivir was then generated using the initial conformation from the crystal structure of zanamivir as a template. Both structures were optimized by the semi-empirical AM1 method in the SPARTAN'04 program [16]. The residues associating in the binding pocket was defined by conserved amino acid residues that are found in all N1, N2 and N9 subtypes which are Arg106, Glu107, Asp139, Arg140, Try167, Arg213, Glu265, Glu266 and Arg281 according to their multiple sequence alignment in figure 1. These residues were also defined as the catalytic site of the NA by Wei *et al.* from difference fourier analysis of crystals soaked in sialic acid [17]. Additionally, their neighbor residues in a radius of 3 Å of these conserved amino acids were selected and defined as the members of the binding pocket. The potential mean force (PMF) scores of the drugs were evaluated by a genetic algorithm with a population size of 50, crossover rate of 0.80, elitism of 5, mutation rate of 0.2 and the maximum cycle generation is set to be 40,000. The size of the grid box is $30 \times 30 \times 30$ Å. Finally, the complex structures were analyzed and the interaction energy between the ligand and protein was calculated.

3. Results and discussion

3.1 Modeling of 3-dimensional structure of H5N1-NA

Multiple sequence alignment of N1-NA and its related sequences were shown in figure 1. These alignments reflect the structurally conserved regions of the available crystal structures. The similarity of N1-NA with N2-NA and N9-NA sequences is about 46 and 49%, respectively. The overall sequence region that MODELLER used to construct the initial model was set at residues 78–457. The rough 3D model (model A) of 380 amino acids was generated and the quality of the model was checked by PROCHECK. Starting from model A, refinement was performed using energy minimization and molecular dynamic in implicit solvent. Then, models A1 and A2 were, respectively, yielded. The quality of the rough and refined models were collected in table 1. There are more residues in core regions of the minimized model than those of MD. Model A1 has the residues of 0.3% in disallowed regions, whereas, model A2 has no residues in disallowed regions. The root mean square displacement (RMSD) of all atoms in A1 and A2 shows insignificant structure difference. The Ramachandran plot of model A2 was illustrated in figure 2. Based on an analysis of 118 structures of resolution of at least 2.0 Å and *R*-factor lower

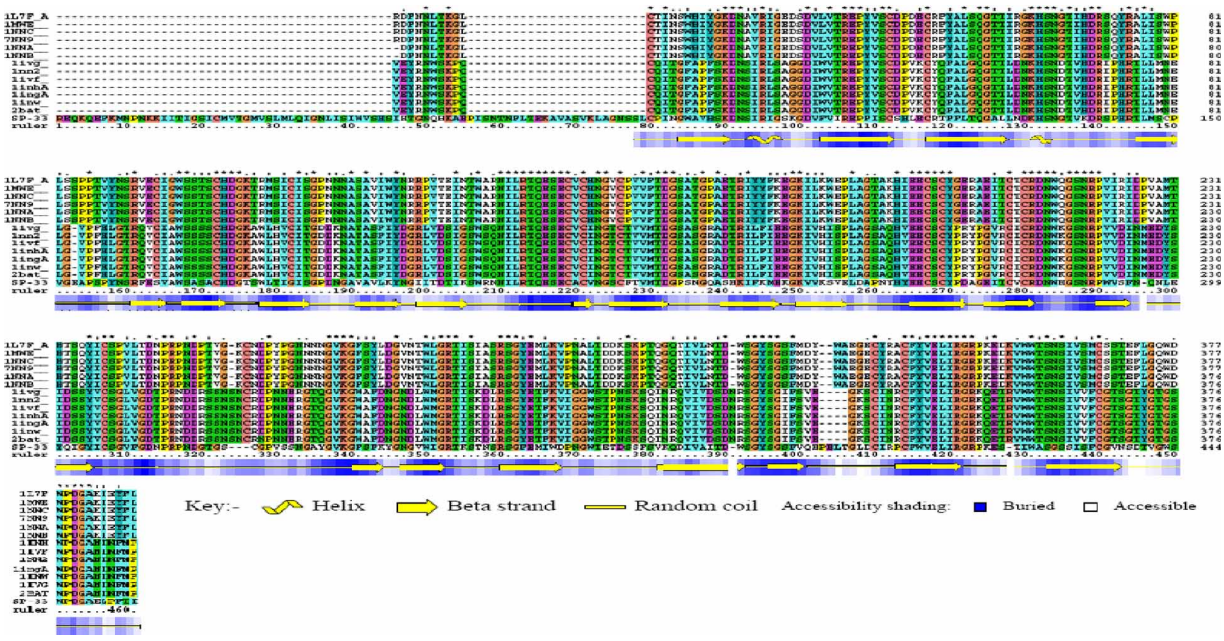

Figure 1. Multiple sequence alignment of H5N1-NA and its related sequences. The secondary structure was predicted by PROCHECK.

than 20%, the results indicate reliability of model A2 in which over 99% of the backbone dihedrals fall within the structurally favorable regions. The decomposition interaction energies (DE)—interaction between residue i and the other $N-1$ residues where N denotes total residues of enzyme—of models A1 and A2 were further checked using PROSA and plotted in figure 3a. It appears that the decomposition energies are almost negative indicating stability of the enzyme. The overall DE of model A2 is lower than that of model A1. Two high DE regions were found in the amino acid range 60–70 and 300–320 for model A1 whereas only the first region was observed for model A2. The above conclusions were confirmed by the results evaluated by the VERIFY3D routine in the Amber program. Here, most of the residues in model A2 falls within the criteria score (>0.1). Inappropriate region, where criteria score >0.1, was observed at residues >360. However, these residues are not in the binding region, and should not affect our enzyme-ligand binding.

3.2 Charge distribution on zanamivir and oseltamivir

The electrostatic charge of zanamivir and oseltamivir were calculated based on the semi-empirical AM1 method using the SPARTAN'04 program. Figure 4 shows the molecular structure and the atomic net charges around the central ring at the positions *a*, *c*, *d* and *e* for the zanamivir and oseltamivir. The charge differences, subtract charges of atoms of zanamivir by those of oseltamivir, at the positions *a*, *c*, *d* and *e* are 0.004, −0.146, 0.256 and 0.168, respectively. This observation leads to the same conclusion for both inhibitors, i.e. the net charges of the —COO, —NH, amide and —R (ether/glycerol) side chains (summation of the atomic net charges of all atoms of each functional group) of zanamivir are similar, less negative, more negative and more negative in comparison, respectively, to those of oseltamivir. The main difference in charge distribution was found on the position *d* and the

Table 1. Quality of the Ramachandran plots for the initial 3D model (A) using PROCHECK and its refinement using energy minimization (model A1) and implicit MD simulation (model A2).

Model	*Ramachandran plot quality (%)*			
	Core	*Allowed*	*General*	*Disallowed*
A	88.1	11.0	0.6	0.3
A1	89.0	10.1	0.6	0.3
A2	81.8	17.6	0.6	0.0

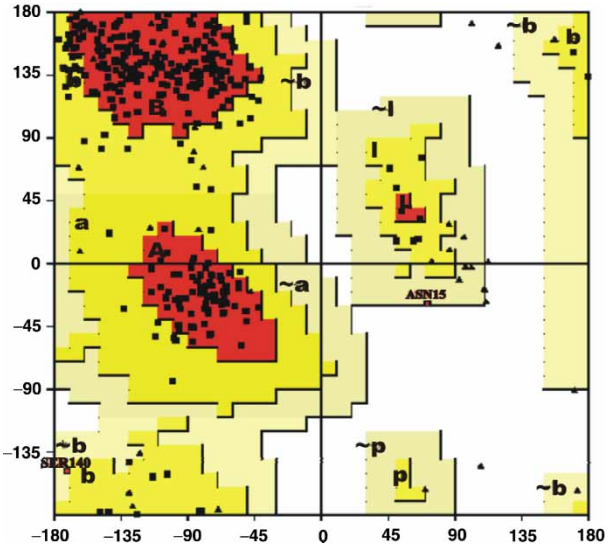

Figure 2. Ramachandran plot of model A2 (see text for more details).

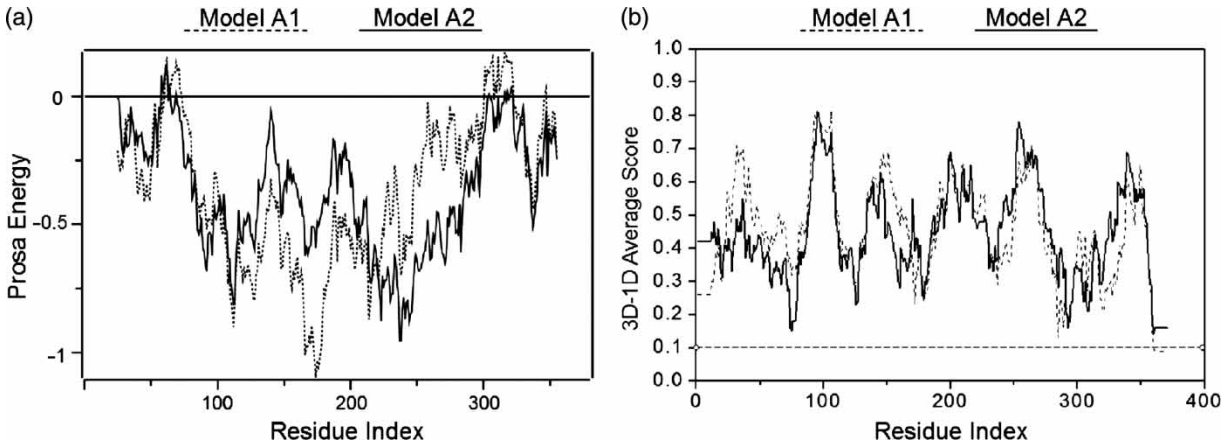

Figure 3. Changes of the Prosa Energy and 3D–1D average score as a function of residue indexes for models A1 (– – – – –) and A2 (– – – – – – – – – – –) (see text for more details).

amide group. Increasing in electron density at *d* and *e* positions as well as the corresponding connected side chains, causes each inhibitor to bind to the amino acids at the binding pocket differently. The details on the complex structure with the complementally hydrophobic and hydrophilic interactions between the side chain and active pocket were discussed in the next section.

3.3 Comparison between N1-NA, N2-NA and N9-NA binding pocket

To understand the drug-resistance of H5N1 virus at a molecular level, zanamivir and oseltamivir were flexible-docked into the binding pocket of the three different neuraminidase subtypes, our N1, N2 (PDB ID: 1IVF) [18] and N9 (PDB ID: 1NNB) models [19]. Amino acid residues lying within 5 Å from ligands were evaluated and reported in table 2. The acidic, basic, polar and nonpolar residues were shown in red, blue, green and black, respectively. It was found that the seven conserved amino acid residues around the active site in all case of N1, N2 and N9 are N1 [Arg29, Glu30, Asp62, Arg63, Glu189, Arg204 and Arg279], N2 [Arg118, Glu119, Asp151, Arg152, Glu277, Arg292 and Arg371] and N9 [Arg119, Glu120, Asp152, Arg153, Glu279, Arg294 and Arg372]. The data shows similarity between binding pockets of N2 and N9. This is also shown by the flexible docking score in table 3.

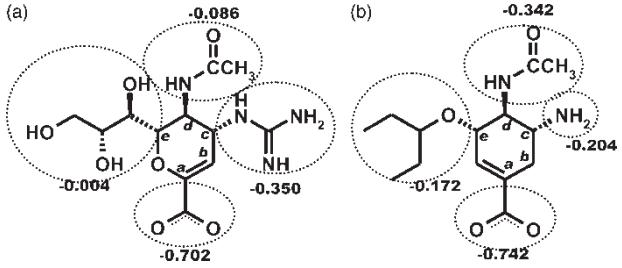

Figure 4. Molecular structure of (a) zanamivir and (b) oseltamivir and summation of the atomic net charges (in atomic unit) for the atoms in the functional group marked by cycle.

In the investigated systems, hydrophobic interactions were found to change docking free energy between ligand and enzyme significantly. The different nonpolar residues (from table 2 and figure 5) were observed, especially around the —COO and —R (ether/glycerol group) of inhibitors, indicating the hydrophobicity difference in facilitating enzyme-ligand binding between the N2/N9 and the N1 pockets. This can be clearly seen by the binding free energy of the complexes shown in table 3 in which those of N1-ligand binding is found to be less potent than N2 and N9 subtypes, while N2-ligand and N9-ligand are roughly comparable. This finding is true for both inhibitors. In addition, it is interesting to observe that binding free energies for all three subtypes of the zanamivir complexes are lower than those of oseltamivir.

In order to monitor the binding environment, the positions of the seven conserved amino acid residues for the three subtypes were mapped to the side chain position of ligands. The results were shown in figure 5. It was found that the zanamivir formed a similar binding pattern to all three subtypes. In contrast, the binding of the —O—R group of oseltamivir in the N1-NA complex was observed to be located at the position different from those of the N2-NA and N9-NA complexes. This indicates higher flexibility of the oseltamivir side chain that can be easier to adapt itself to the new environment, and hence, lower its resistance to enzyme mutation in comparison to those events of zanamivir.

3.4 N1-Neuraminiase and ligand binding from flexible docking

To correctly identify the most favorable binding interaction that ligand poses from a set of energetically reasonable conformations and orientations, the flexible molecular docking has been performed with the genetic algorithm. With this method, it allows both the ligand and the binding pocket to be flexible during the calculation to optimize the interactions. Oseltamivir and zanamivir were docked to the N1-NA binding site. Figure 6a,b show

Table 2. Numbers and types of residues which were detected at the binding pockets of the N1-NA, N2-NA and N9-NA complexed with zanamivir and oseltamivir.

Zanamivir			*Oseltamivir*		
N1 subtype	*N2 subtype†*	*N9 subtype†*	*N1 subtype*	*N2 subtype†*	*N9 subtype†*
(1) Arg29 (a,e)	**(1) Arg118** (e)	**(1) Arg119** (e)	**(1) Arg29** (c)	**(1) Arg118** (a)	**(1) Arg119** (c)
(2) Glu30 (a)	**(2) Glu119** (e)	**(2) Glu120** (c,e)	**(2) Glu30** (c,d)	**(2) Glu119** (c)	**(2) Glu120** (c)
		Ile150 (e)	Lys61 (d)		
(3) Asp62 (d)	**(3) Asp151** (d,e)	**(3) Asp152** (c,e)	**(3) Asp62** (d)	**(3) Asp151** (c)	**(3) Asp152** (c,d)
(4) Arg63 (c,d)	**(4) Arg152** (a,c)	**(4) Arg153** (e)	**(4) Arg63** (c,d)	**(4) Arg152** (c)	**(4) Arg153** (d)
	Arg156 (c)	Arg157 (e)	Arg67 (d)	Arg156 (c)	Arg157 (c)
	Trp178 (c)	Trp180 (e)		Trp178 (c,d)	Trp180 (d)
	Ser179 (c)	Ser181 (e)		Ile222 (e)	Ser181 (d)
	Ile222 (a)	Ile224 (a)		Arg224 (d,e)	Ile224 (e)
	Arg224 (c,d)	Arg226 (c,d)		Thr225 (d)	Arg226 (e)
	Thr225 (c,d)	Glu229 (c)		Glu227 (c,d)	Glu229 (d)
	Glu227 (c,d)	Ala248 (d)		Ala246 (e)	Ala248 (e)
	Ala246 (a)	Glu278 (d)		Glu276 (d,e)	Glu278(e)
	Glu276 (c)				
(5) Glu189 (c)	**(5) Glu277** (c)	**(5) Glu279** (d)		**(5) Glu277** (d)	**(5) Glu279** (d)
(6) Arg204 (c)	**(6) Arg292** (d,e)	**(6) Arg294** (d)	**(6) Arg204** (a,c)	**(6) Arg292** (e)	**(6) Arg294** (e)
Gly256 (c)	Gly348 (e)	Asn296 (d)		Asn94 (e)	Asn296 (e)
		Asn348 (e)			Asn348 (a,e)
		Gly349 (e)			
(7) Arg279 (a)	**(7) Arg371** (e)	**(7) Arg372** (e)	**(7) Arg279** (a)	**(7) Arg371** (a)	**(7) Arg372** (a)
Trp310 (e)	Tyr406 (e)	Tyr406 (e)	Trp310 (e)	Tyr406 (a,c)	Tyr406 (a,c)
Ser311 (a,e)			Tyr313 (a)		
Gly312 (a)			Glu336 (a)		
Tyr313 (a)			Ile338 (a,e)		
Glu336 (a)			Trp348 (e)		
Ile338 (a,e)			Ala349 (e)		
Arg341 (e)					
Trp348 (e)					
Ala349 (e)					

The acidic, basic, polar and nonpolar residues were shown in red, blue, green and black, respectively.† The amino acid residue numbers are from the X-ray structure. The residues (1)–(7) are the seven conserved amino acid commonly found in all cases. *a*, *c*, *d* and *e* in parenthesis indicated the ligand binding position according to figure 4.

schematic illustrations representing interactions between the two inhibitors and the active site residues of N1-NA. The final scores of the lowest free energy are −118.492 and −109.715 kcal/mol (table 3) for zanamivir and oseltamivir, respectively. To relate the calculated PMF score to an absolute binding free energy a scaling factor should be used as ΔG_{bind} = PMF score/scaling factor [13]. Although, no test set for H5N1 model has not yet been reported, an approximate scaling factor in order of 10 magnitudes should be applied and the *Ki* are found to be in the *nM* range. As can be seen from the figures that common amino acids which facilitate the enzyme-ligand binding within 5 Å from both drugs are Arg29, Glu30, Asp62, Arg63, Arg204, Arg279, Trp310, Tyr313, Glu336, Ile338, Trp348 and Ala349. The amino acids associated within 5 Å from atoms of zanamivir only are Glu189, Gly256, Ser311, Gly312 and Arg341 while those found only for oseltamivir are Lys61 and Arg67. More hydrophilic basic residues found in oseltamivir case, as also reported in table 3, leads to the higher negative charge at position *c* and *d* in figure 4. This was also discussed earlier in Section 3.3.

Table 3. Flexible docking free energy of binding for the two investigated inhibitors in the binding pocket of N1-NA, N2-NA and N9-NA subtypes.

Complex	*Free energy (kcal/mol)*
Zanamivir + N1-NA	−118.492
Zanamivir + N2-NA	−145.072
Zanamivir + N9-NA	−138.374
Oseltamivir + N1-NA	−109.715
Oseltamivir + N2-NA	−123.114
Oseltamivir + N9-NA	−122.251

Accordingly, in the complex of N1-NA with zanamivir, the glycerol side chain with a partial hydrophobic group is fixed tightly by three hydrogen bonds with Arg29–NH at O-hydroxyl group of the glycerol side chain. Another

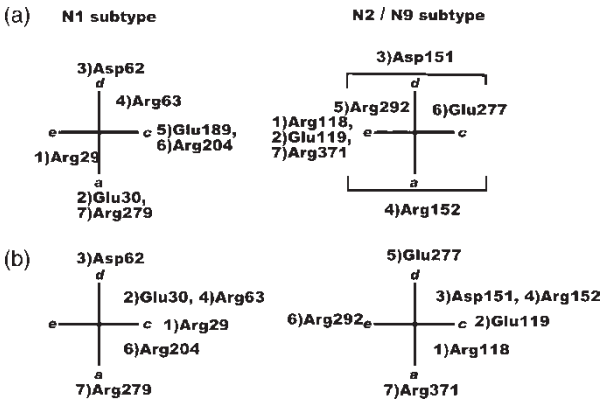

Figure 5. The key amino acid residues in the binding pocket of N1 and N2 or N9 located within 5 Å from atoms of (a) zanamivir and (b) oseltamivir.

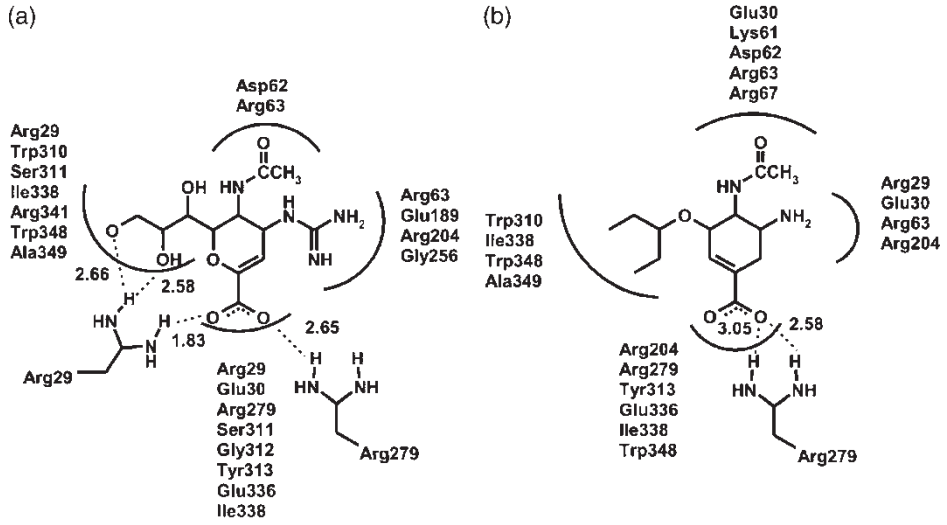

Figure 6. Schematic illustrations to show the binding interactions of the (a) zanamivir and (b) oseltamivir with H5N1-NA. The dotted lines represent the hydrogen bond where the corresponding hydrogen bond distances (in Å) were also given.

hydrogen bond was detected between Arg279–NH and the O-carboxyl group of zanamivir. A stronger bond is formed between Arg29–NH and O-carboxyl with a distance of 1.83 Å. Therefore, the hydrogen bonds between Arg29 and the hydroxyl group of the glycerol side chain might block the hydrophobic interaction between the carbon and the hydrocarbon chain of the surrounding amino acids. More difficulty in adjusting the position of the glycerol group to the change in the hydrophobic environment in the N1-NA would be expected.

In addition, in contrast to what is detected for zanamivir, the —O—R group at the position *e* (figure 4) in oseltamivir was found to replace the glycerol side chain. This side chain has a lower steric effect from the hydroxyl groups so that it can easier rotate the single bond between the oxygen and the alkyl chain R in the partial hydrophobic pocket. As a result, the positions of conserved amino acids indexed 1–7 binding to each *a*–*e* side chains of oseltamivir are changed whereas those of zanamivir are mostly fixed as a mutation occurs from N1 to N2 or N9 as shown in figure 5. Only two hydrogen bonds, which are not associated with the side chain interactions, between Arg279–NH and O-carboxyl are formed. This data indicates that oseltamivir is able to adapt itself to the change of hydrophobic environment in the N1-NA pocket. This is fully consistent with that observed by Mase *et al.* [20] that the particular H5N1-NA did show sensitivity to oseltamivir. The complementally hydrophobic and hydrophilic interactions between the side chain at the position *e* and active pocket are determining the inhibiting activity.

4. Conclusion

Three dimensional structure models of neuraminidase H5N1 isolated from Thailand were constructed by homology modeling with the 13 high-resolution X-ray structures of neuraminidase N2 and N9. The best refinement model was derived from implicit solvent MD simulation. The overall quality of this model was evaluated by PROCHECK, PROSA and VERIFY3D. The reliability of the obtained model was shown by the Ramachandran plot in which 81.8, 17.6, 0.6 and 0.0% of the residues are in the most favored region, additional allowed regions, generously allowed regions and disallowed region, respectively. Meanwhile, the results from the PROSA and VERIFY3D are all well within their criteria. Evaluation scores from these tests confirm that this model is an adequate one for further investigation. Flexible docking studies of the two drugs show the complementary hydrophobic and hydrophilic environments between enzyme and drugs. In some cases, specific mutations have been associated with drug resistance. However, the flexibility of the —O—R group in oseltamivir complex leads to the lower drug-resistance to enzyme mutation in the more hydrophobic pocket of N1 in comparison to those of N2 and N9. The hydrophobicity of the inhibitors is not only an important factor for determining the inhibitory activity but also for designing orally active drugs. Such a finding might provide the information for designing new drugs against these viruses.

Acknowledgements

This work is supported by grants from the Thailand Research Funding (TRF) and National Center for Genetic Engineering and Biotechnology (BIOTEC), Postgraduate Education and Research Program in Chemistry: Center of Innovation in Chemistry (PERCH-CIC), Thailand and also supported by the computer simulation and modeling research laboratory (CSML), Department of Chemistry, Chiang Mai University. The authors also thank the anonymous reviewers whose comments were very helpful to make the presentation of this study more accurate.

References

[1] K. Subbarao, A. Klimov, J. Katz, H. Regnery, W. Lim, H. Hall, M. Perdue, D. Swayne, C. Bender, J. Huang, M. Hemphill, T. Rowe, M. Shaw, X. Xu, K. Fukuda, N. Cox. Characterization of an avian influenza A (H5N1) virus isolated from a child with a fatal respiratory illness. *Science*, **279**, 393 (1998).

[2] T. Horimoto, Y. Kawaoka. Pandemic threat posed by avian influenza A viruses. *Clin. Microbiol. Rev.*, **14**, 129 (2001).

[3] B.J. Smith, P.M. Colman, M. Von Itzstein, B. Danylec, J.N. Varghese. Analysis of inhibitor binding influenza virus neuraminidase. *Protein Sci.*, **10**, 689 (2001).

[4] C. Liu, M.C. Eichelberger, R.W. Compans, G.M. Air. Influenza type A virus neuraminidase does not play a role in viral entry, replication, assembly, or budding. *J. Virol.*, **69**, 1099 (1995).

[5] P. Puthavathana, P. Auewarakul, P.C. Charoenying, K. Sangsiriwut, P. Pooruk, K. Boonnak, R. Khanyok, P. Thawachsupa, R. Kijphati, P. Sawanpanyalert. Molecular characterization of the complete genome of human influenza H5N1 virus isolates from Thailand. *J. Gen. Virol.*, **86**, 423 (2005).

[6] J.D. Thompson, T.J. Gibson, F. Plewniak, F. Jeanmougin, D.G. Higgins. The CLUSTAL_X windows interface: flexible strategies for multiple sequence alignment aided by quality analysis tools. *Nucleic Acids Res.*, **25**, 4876 (1997).

[7] A. Sali, T.L. Blundell. Comparative protein modelling by satisfaction of spatial restraints. *J. Mol. Biol.*, **234**, 779 (1993).

[8] D.A. Case, T.A. Darden, T.E. Cheatham III, C.L. Simmerling, J. Wang, R.E. Duke, R. Luo, K.M. Merz, B. Wang, D.A. Pearlman, M. Crowley, S. Brozell, V. Tsui, H. Gohlke, J. Mongan, V. Hornak, G. Cui, P. Beroza, C. Schafmeister, J.W. Cadwell, W.S. Ross, P.A. Kollman. *AMBER 8*, San Francisco, University of California (2004).

[9] D.A. Pearlman, D.A. Case, J.W. Caldwell, W.S. Ross, T.E. Cheatham III, S. DeBolt, D. Ferguson, G. Seibel, P. Kollman. AMBER, a package of computer programs for applying molecular mechanics, normal mode analysis, molecular dynamics and free energy calculations to simulate the structural and energetic properties of molecules. *Comp. Phys. Commun.*, **91**, 1 (1995).

[10] R.A. Laskowski, M.W. MacArthur, D.S. Moss, J.M. Thornton. PROCHECK: a program to check the stereo chemical quality of protein structures. *J. Appl. Cryst.*, **26**, 283 (1993).

[11] M.J. Sippl. Boltzmann's principle, knowledge based mean fields and protein folding, an approach to the computational determination of protein structures. *J. Comput. Aided Mol. Design*, **7**, 473 (1993).

[12] R. Luthy, J.U. Bowie, D. Eisenberg. Assessment of protein models with three-dimensional profiles. *Nature*, **356**, 83 (1992).

[13] I. Muegge, Y.C. Martin. A general and fast scoring function for protein–ligand interactions: a simplified potential approach. *J. Med. Chem.*, **42**, 791 (1999).

[14] BioMedCache 2.0, CAChe work system pro 6.1, Fujitsu, Inc. CAChe Group. Fujitsu, 1250 E, Arques Avenue, Sunnyvale, CA 94085, USA.

[15] N.R. Taylor, A. Cleasby, O. Singh, T. Skarzynski, A.J. Wonacott, P.W. Smith, S.L. Sollis, P.D. Howes, P.C. Cherry, R. Bethell, P. Colman, J. Varghese. Dihydropyrancarboxamides related to zanamivir: a new series of inhibitors of influenza virus sialidases. 2. Crystallographic and molecular modeling study of complexes of 4-amino-4H-pyran-6-carboxamides and sialidase from influenza virus types A and B. *J. Med. Chem.*, **41**, 798 (1998).

[16] Spartan'04 Windows. Wavefunction, Inc., 18401 Von Karman Avenue, Suite 370, Irvine, CA 92612, USA.

[17] D.Q. Wei, Q.S. Du, H. Sun, K.C. Chou. Insights from modeling the 3D structure of H5N1 influenza virus neuraminidase and its binding interactions with ligands. *Biochem. Biophys. Res. Commun.*, **344**, 1048 (2006).

[18] M.J. Jedrzejas, S. Singh, W.J. Brouillette, W.G. Laver, G.M. Air, M. Luo. Structures of aromatic inhibitors of influenza virus neuraminidase. *Biochemistry*, **34**, 3144 (1995).

[19] P. Bossart-Whitaker, M. Carson, Y.S. Babu, C.D. Smith, W.G. Laver, G.M. Air. Three-dimensional structure of influenza A N9 neuraminidase and its complex with the inhibitor 2-deoxy 2,3-dehydro-*N*-acetyl neuraminic acid. *J. Mol. Biol.*, **232**, 1069 (1993).

[20] P.M. Colman, W.R. Tulip, J.N. Varghese, P.A. Tulloch, A.T. Baker, W.G. Laver, G.M. Air, R.G. Webster. Three-dimensional structures of influenza virus neuraminidase-antibody complexes. *Philos. Trans. R. Soc. Lond. B Biol. Sci.*, **323**, 511 (1989).